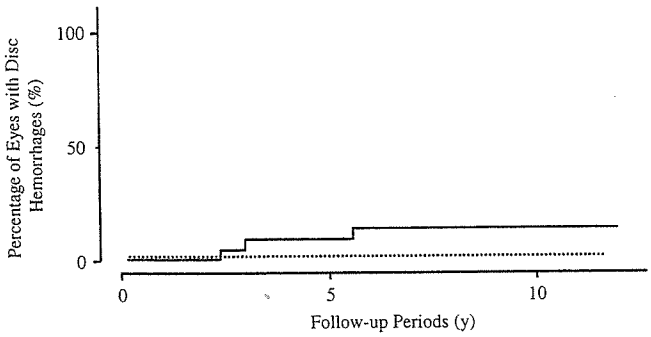

FIGURE 3. The cumulative probability of detecting disc hemorrhages after trabeculectomy over time in the high and the low postoperative IOP subgroups (POAG) by the Kaplan-Meier analysis. The solid line indicates the high postoperative IOP group and the dotted line represents the low postoperative IOP group. The probability in the low and the high postoperative group was 1.4 ± 1.4% and 13.6 ± 7.4%, respectively (calculated probability ± SE). The final cumulative probability of detecting disc hemorrhages over time in the high postoperative IOP group was higher than that in the low postoperative IOP group ($P = 0.0393$, log-rank test).

et al[21] studied the alterations in the incidence of disc hemorrhages resulting after ocular hypotensive therapy. Although IOP in NTG patients went down approximately 2 mm Hg from baseline, they found that there were no changes in the incidence of disc hemorrhages before and after treatment in NTG patients. Whereas in POAG patients and glaucoma suspects, they reported that the incidence of disc hemorrhages significantly decreased after therapy with IOP reduction (POAG: 23.9 to 18.8 mm Hg; glaucoma suspects: 22.3 to 18.4 mm Hg). However, the difference of our results in this study (POAG: 19.6 to 11.1 mm Hg; NTG: 15.3 to 11.3 mm Hg) from theirs could be due to a much smaller lowering of IOP in their groups.

In our previous report,[38] we documented that the incidence of disc hemorrhages in 32 trabeculectomized NTG eyes was 43.8% (14/32) postoperatively, as opposed

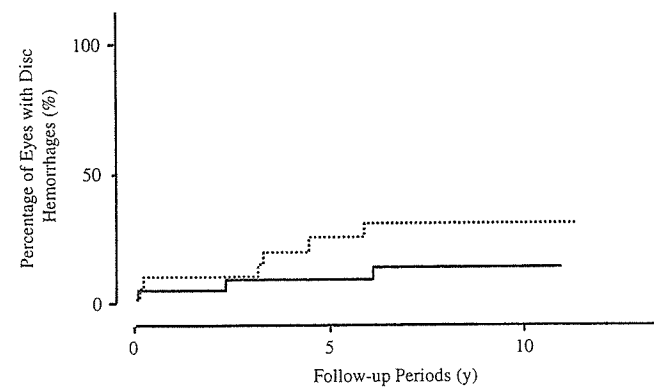

FIGURE 4. The cumulative probability of detecting disc hemorrhages after trabeculectomy over time in the high and the low postoperative IOP subgroups (NTG) by the Kaplan-Meier method. The solid line indicates the high postoperative IOP group and the dotted line represents the low postoperative IOP group. The probability in the low and the high postoperative group was 29.2 ± 10.2% and 12.4 ± 6.8%, respectively (calculated probability ± SE). Unlike POAG, the cumulative probability of detecting disc hemorrhages over time in the high postoperative IOP group was lower than that in the low postoperative IOP group ($P = 0.1750$, log-rank test).

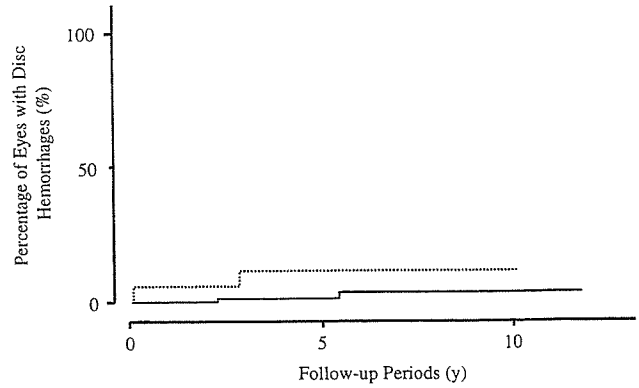

FIGURE 5. The cumulative probability of detecting disc hemorrhages after trabeculectomy over time in the preoperative disc hemorrhage-positive and hemorrhage-negative subgroups (POAG) by the Kaplan-Meier analysis. The solid line indicates the disc hemorrhage-negative group and the dotted line represents the disc hemorrhage-positive group. The probability in the disc hemorrhage-negative and hemorrhage-positive group was 3.5 ± 2.5% and 11.9 ± 7.9%, respectively (calculated probability ± SE). The cumulative probability of detecting the disc hemorrhage over time in the disc hemorrhage-positive group was higher than that in the disc hemorrhage-negative group. ($P = 0.0617$, log-rank test).

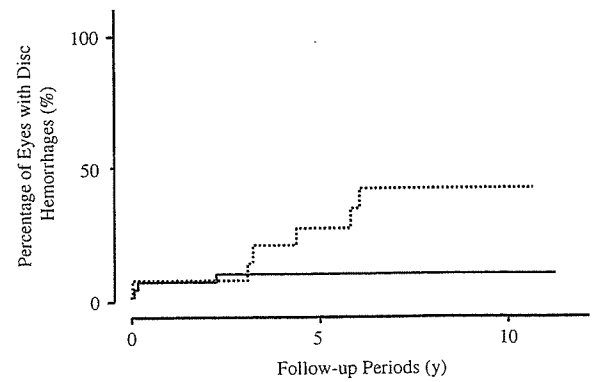

FIGURE 6. The cumulative probability of detecting the disc hemorrhage after trabeculectomy over time in the preoperative disc hemorrhage-positive and hemorrhage-negative subgroups (NTG) by the Kaplan-Meier method. The solid line indicates the disc hemorrhage-negative group and the dotted line represents the disc hemorrhage-positive group. The probability of the disc hemorrhage-negative and hemorrhage-positive group was 8.9 ± 4.9% and 41.1 ± 13.0%, respectively (calculated probability ± SE). There was a statistically significant difference between the two groups ($P = 0.0225$, log-rank test).

to a postoperative incidence of 12.5% (4/32). We also suggested that a significant postoperative IOP reduction might alleviate the worsening of the visual field indices. In the present study, we confirmed that lowering IOP via surgical intervention might lead to the lower incidence of disc hemorrhages in large populations of OAG including POAG.

One remaining and interesting question is to determine why patients with lowered IOP are less likely to develop an optic disc hemorrhage. With regard to the etiology of glaucomatous optic neuropathy, conflicting arguments still exist between a mechanical theory, which focuses on the mechanical compression on the optic nerve head due to IOP, and a circulatory disorder theory whereby deformation of the lamina cribrosa or optic nerve disorder is believed to follow a circulatory perturbation of the lamina cribrosa. Our results are consistent with decreased incidence of disc hemorrhage after filtering surgery via either one or both of (1) direct action of the postoperative lowered IOP and (2) amelioration of blood circulation around the optic nerve head secondary to decreased postoperative IOP.

Interestingly, our present study further documented that in POAG eyes the high postoperative IOP group had a statistically significant higher incidence of disc hemorrhages than the low postoperative IOP group, and that, conversely, in NTG eyes the former group tended to have a higher incidence of disc hemorrhages than the latter group. Furthermore, in both POAG and NTG subgroups eyes with disc hemorrhages preoperatively tended to rebleed postoperatively despite the relatively lowered postoperative IOP via surgical intervention. According to previous literatures that describe the relationship between IOP without surgical intervention and disc hemorrhages, Krakau[39] or Gloster[30] revealed a high incidence of disc hemorrhages in a group of patients with an IOP of 18 to 20 mm Hg or 11 to 20 mm Hg, respectively. Additionally, Slight[40] reported that in 90% (32/36) of eyes with disc hemorrhages, their IOPs were 25 mm Hg or less. On the other hand, Drance et al[41] showed that IOPs in the disc hemorrhage group were low in comparison with those without disc hemorrhage. Our results indicated that NTG eyes seemed to have more complicated etiology than POAG eyes, although in at least even subsets of NTG eyes with IOP reduction via trabeculectomy could markedly inhibit the detection of disc hemorrhages. However, we need to seek a rational explanation for the decrease in the incidence of disc hemorrhages despite lowered postoperative IOP, especially in NTG eyes.

This study has several limitations, including nonstandardized follow-up and selection bias, because of its retrospective nature. Further, the sample size of the 2 groups was small, especially that of the NTG group, and unequal. Therefore, although it is difficult to draw a conclusion based on our results, we believe that our results were of substantial magnitude and could be real.

In summary, in the current study we confirmed that the incidence of disc hemorrhages decreased in both NTG and POAG patients who underwent trabeculectomy. However, both POAG and NTG subgroup eyes with disc hemorrhages preoperatively tended to show reappearance of disc hemorrhages postoperatively regardless of relatively reduced postoperative IOP via surgical intervention. The exact underlying mechanisms by which glaucomatous optic neuropathy would develop or progress remains unclear and requires further studies.

REFERENCES

1. Bjerrum. Om en teillfojelse til den saedvanliga synsfeltsundersogelse samt om synsfelt ved glaukom. *Nord Ophthalmol Tidskr.* 1889;2: 141–185.
2. Drance SM, Begg IS. Sector hemorrhage—a probable acute ischemic disc change in chronic simple glaucoma. *Can J Ophthalmol.* 1970;5:137–141.
3. Sugiyama K, Tomita G, Kitazawa Y, et al. The associations of optic disc hemorrhage with retinal nerve fiber layer defect and peripapillary atrophy in normal-tension glaucoma. *Ophthalmology.* 1997;104:1926–1933.
4. Shirato S, Koseki N. Disc hemorrhage in low-tension glaucoma. In: Krieglstein GK, ed. *Glaucoma Update IV.* Berlin: Springer-Verlag; 1991:125–128.
5. Diehl DLC, Quigley HA, Miller NR, et al. Prevalence and significance of optic disc hemorrhage in a longitudinal study of glaucoma. *Arch Ophthalmol.* 1990;108:545–550.
6. Drance SM. Disc hemorrhages in the glaucomas. *Surv Ophthalmol.* 1989;33:331–337.
7. Shihab ZM, Lee PF, Hay P. The significance of disc hemorrhage in open-angle glaucoma. *Ophthalmology.* 1982;89:211–213.
8. Susanna R, Drance SM, Douglas GR. Disc hemorrhages in patients with elevated intraocular pressure: occurrence with and without field changes. *Arch Ophthalmol.* 1979;97:284–285.
9. Drance SM. Hemorrhage on disc—a risk factor in glaucoma. In: Krieglstein GK, Leydhecker W, eds. *Glaucoma Update II.* Berlin: Springer-Verlag; 1983:77–79.
10. Siegner SW, Netland PA. Optic disc hemorrhages and progression of glaucoma. *Ophthalmology.* 1996;103:1014–1024.
11. Ishida K, Yamamoto T, Sugiyama K, et al. Disk hemorrhage is a significantly negative, prognostic factor in normal-tension glaucoma. *Am J Ophthalmol.* 2000;129:707–714.
12. Ishida K, Yamamoto T, Kitazawa Y. Clinical factors associated with the progression of normal-tension glaucoma. *J Glaucoma.* 1998;7:372–377.
13. Raster MT, Enden A, Bakker DB, et al. Deterioration of visual fields in patients with glaucoma with and without optic disc hemorrhages. *Arch Ophthalmol.* 1997;115:1257–1263.
14. Begg IS, Drance SM, Sweeney VP. Ischemic optic neuropathy in chronic simple glaucoma. *Br J Ophthalmol.* 1971;55:73–90.
15. Sugiyama K, Cioffi GA, Bacon DR, et al. Optic Nerve and peripapillary choroidal microvasculature in the primate. *J Glaucoma.* 1994;3:45–54.
16. Quigley HA, Addicks EM, Green WR, et al. Optic nerve damage in human glaucoma. *Arch Ophthalmol.* 1981;99:635.
17. Kitazawa Y. Open-angle glaucoma clinical presentation and management. *J Jpn Ophthalmol Soc.* 2001;105:828–842.
18. Drance S, Anderson DR, Schulzer M, for the Collaborative Normal-Tension Glaucoma Study Group. Risk factors for progression of visual field abnormalities in normal-tension glaucoma. *Am J Ophthalmol.* 2001;131:699–708.
19. Collaborative NTG Study Group. Comparison of glaucomatous progression between untreated patients with NTG and patients with therapeutically reduced IOP. *Am J Ophthalmol.* 1998;126:487–497.
20. Collaborative NTG Study Group. The effectiveness of IOP reduction in the treatment of NTG. *Am J Ophthalmol.* 1998;126: 498–505.
21. Hendrickx KH, van den Enden A, Rasker MT, et al. Cumulative incidence of patients with disc hemorrhages in glaucoma and the effect of therapy. *Ophthalmology.* 1994;101:1165–1172.

22. Kitazawa Y, Kawase K, Matsushita H, et al. Trabeculectomy with mitomycin C (a comparative study with fluorouracil). *Arch Ophthalmol.* 1991;109:1693–1698.
23. Quigley HA, Maumenee AE. Long-term follow-up of treated open-angle glaucoma. *Am J Ophthalmol.* 1979;87:519–525.
24. Grant WM, Burke JF Jr. Why do some people go blind from glaucoma?. *Ophthalmology.* 1982;89:991–998.
25. Odberg T. Visual field prognosis in advanced glaucoma. *Acta Ophthalmol.* 1987;65:27–29.
26. American Academy of Ophthalmology. Preferred Practice Patterns TM. *Open-Angle Glaucoma.* 2000;38.
27. Kitazawa Y, Shirato S, Yamamoto T. Optic disc hemorrhage in low-tension glaucoma. *Ophthalmology.* 1986;93:853–857.
28. Bengtsson B, Holmin C, Krakau CET. Disc hemorrhage and glaucoma. *Acta Ophthalmol.* 1981;59:1–14.
29. Hoyng PFJ, de Jong N, Oosting H, Stilma J. Platelet aggregation, disc hemorrhage and progressive loss of visual fields in glaucoma. *Int Ophthalmol.* 1992;16:65–73.
30. Gloster J. Incidence of optic disc haemorrhages in chronic simple glaucoma and ocular hypertension. *Br J Ophthalmol.* 1981;65:452–456.
31. Holmin C. Signs of activity and progression in chronic glaucoma. *Acta Ophthalmol.* 1982;153:1–40.
32. Bengtsson B. Findings associated with glaucomatous visual field defects. *Acta Ophthalmol.* 1980;58:20–32.
33. Drance SM, Sweeney VP, Morgan RW, et al. Studies of factors involved in the production of low tension glaucoma. *Arch Ophthalmol.* 1973;89:457–465.
34. Levene RZ. Low tension glaucoma: a critical review and new material. *Surv Ophthalmol.* 1980;24:621–664.
35. Chumbley LC, Brubaker RF. Low-tension glaucoma. *Am J Ophthalmol.* 1976;81:761–767.
36. Jonas JB, Xu L. Optic disk hemorrhages in glaucoma. *Am J Ophthalmol.* 1994;118:1–8.
37. Sonnsjo B, Holmin C, Krakau CE. Occurrence of disc haemorrhages in open-angle glaucoma treated with pilocarpine or timolol. *Acta Ophthalmol.* 1991;69:217–224.
38. Daugeliene L, Yamamoto T, Kitazawa Y. Effect of trabeculectomy on visual field in progressive normal-tension glaucoma. *Jpn J Ophthalmol,* 1998;42:286–292.
39. Krakau CET. Disc hemorrhages: Forerunners of chronic glaucoma. In: Krieglstein GK, Leydhecker W, eds. *Glaucoma Update II.* Berlin: Springer Verlag; 1983:71–76.
40. Slight JR. The significance of disk hemorrhages: A red flag sign. *Trans Pac Coast Oto-ophthalmol Soc.* 1981;62: 25–33.
41. Drance SM, Fairclough M, Butler DM, et al. The importance of disc hemorrhage in the prognosis of chronic open angle glaucoma. *Arch Ophthalmol.* 1977;95:226–228.

BRAIN RESEARCH 1085 (2006) 33-42

available at www.sciencedirect.com

SCIENCE DIRECT

www.elsevier.com/locate/brainres

BRAIN RESEARCH

Research Report

Intraocular injection of folate antagonist methotrexate induces neuronal differentiation of embryonic stem cells transplanted in the adult mouse retina

Akira Hara[a,*], *Masayuki Niwa*[b,c], *Masako Kumada*[d], *Hitomi Aoki*[e], *Takahiro Kunisada*[e], *Takeru Oyama*[a], *Tetsuya Yamamoto*[d], *Osamu Kozawa*[b], *Hideki Mori*[a]

[a]*Department of Tumor Pathology, Gifu University School of Medicine, 1-1 Yanagido, Gifu 501-1194, Japan*
[b]*Department of Pharmacology, Gifu University School of Medicine, 1-1 Yanagido, Gifu 501-1194, Japan*
[c]*Medical Education Development Center, Gifu University School of Medicine, 1-1 Yanagido, Gifu 501-1194, Japan*
[d]*Department of Ophthalmology, Gifu University School of Medicine, 1-1 Yanagido, Gifu 501-1194, Japan*
[e]*Department of Tissue and Organ Development, Gifu University Graduate School of Medicine, 1-1 Yanagido, Gifu 501-1194, Japan*

ARTICLE INFO

Article history:
Accepted 20 February 2006
Available online 11 April 2006

Keywords:
Embryonic stem cell
Methotrexate
Neuronal differentiation
Retina

ABSTRACT

Transplanted embryonic stem (ES) cells can be integrated into the retinas of adult mice as well-differentiated neuronal cells. However, the integrated ES cells also have a tumorigenic effect just because they have the ability for multipotential differentiation to various types of tissues. Thus, control of neoplastic potentials of ES cells is very important for the treatment of degenerative or injured diseases. Mouse ES cells carrying the sequence for the green fluorescent protein (GFP) gene were transplanted into adult mouse retinas by intravitreal injections 20 h after intravitreal N-methyl-D-aspartate (NMDA) administration. One week after the ES cell injection, folate antagonist methotrexate (MTX) was injected intravitreally. Eyes were retrieved 4 weeks after ES cell transplantation for histologic analyses. Conventional histological analysis was performed by hematoxylin and eosin staining with the use of paraffin-embedded sections. Neuronal differentiation and teratogenic potential of ES cells were demonstrated by immunohistochemistry. The proliferative activity of transplanted cells was detected by mitotic index, proliferating cell nuclear antigen index and AgNOR count. The incorporation of transplanted ES cells in MTX-treated and non-treated retinas at 4 weeks after transplantation was observed in 8/16 eyes (50%) and 8/16 eyes (50%), respectively. Transplanted ES cells in MTX-treated retina showed increased neuronal differentiation and decreased expression of teratogenic markers, compared with ES cells in non-treated retina. The proliferative activity of transplanted ES cells in MTX-treated retina was lower than that in non-treated retina. These results suggest that intravitreal MTX treatment following transplantation can induce neuronal differentiation in the transplanted ES cells and decrease their proliferative activity.

* *Corresponding author.* Fax: +81 58 230 6226.
E-mail address: ahara@cc.gifu-u.ac.jp (A. Hara).

0006-8993/$ – see front matter © 2006 Elsevier B.V. All rights reserved.
doi:10.1016/j.brainres.2006.02.079

1. Introduction

Embryonic stem (ES) cells derived from the inner cell mass of blastocyst represent a valuable source for cell-replacement therapy since their characteristic features include an unlimited self-renewing capacity and a multilineage differentiation potential (Doetschman et al., 1985; Resnick et al., 1992; Thomson et al., 1998). The differentiation of ES cells into an intended lineage can be exclusively demonstrated in vitro by the addition of growth factors or induction substances (Okabe et al., 1996; Soria et al., 2001). On the contrary, in vivo application of undifferentiated ES cells into immune-deficient mice produces teratomas comprised of many cell types, demonstrating the pluripotency of the cells (Bieberich et al., 2004). Although ES cells may be attractive candidates for the cell-replacement therapy of various degenerative diseases in the future, the major limitation of its application to this therapy is teratoma formation. For example, ES-cell-derived insulin-producing cells transplanted into diabetic mice produced immature teratomas after transient recovery of hyperglycemia (Fujikawa et al., 2005). Even neural precursor cells derived from ES cells show the unlimited self-renewal and high differentiation potential and have the risk of tumor induction after engraftment (Arnhold et al., 2004).

Neural progenitor cells that give rise to neurons and glia have been identified in different regions of the brain, including the embryonic retina (Ahmad et al., 2004). Recently, such cells have been reported to be present, in a mitotically quiescent state, in the ciliary epithelium of the adult mammalian eye. However, the application of these neural progenitor cells to cell-replacement therapy is limited because of an insufficiency of suitable cell populations that can be transplanted into the vitreous chamber for the retinal reconstruction (Pressmar et al., 2001; Warfvinge et al., 2001; Wojciechowski et al., 2002). On the other hand, these cell populations can be obtained in huge quantities by differentiating embryonic stem cells into the respective cell types, thus making cell-replacement therapies more plausible (Aoki et al., 2006; Arnhold et al., 2004; Haruta et al., 2004; Meyer et al., 2004, 2006). Transplanted undifferentiated ES cells can be integrated into the retinas of adult mice as well-differentiated neuronal cells. However, the integrated ES cells also have a tumorigenic effect just because they have the ability for multipotential differentiation to various types of tissues. Why ES cells, which lack chromosomal abnormalities, possess tumor-like properties is largely unknown. Recently, the transforming oncogene ERas, a Ras-like gene, is reported to be important in the tumor-like growth properties of ES cells (Takahashi et al., 2003), however, therapeutic usage of ES cells is still uncertain. Thus, more care must be taken before using ES cell transplantation as a therapeutic option for patients with degenerative or injured disease, and the control of neoplastic potentials of ES cells is very important for the treatments in the future (Arnhold et al., 2004).

Neuronal differentiation was demonstrated as ganglion-cell-like differentiated ES cells growing along the host retinal surface of adult mouse eye in our previous study (Hara et al., 2004b). Differentiated ES cells, expressing retinal and neuronal markers, developed fine neuronal cell processes around cell nuclei and generated neuronal networks into the retinal inner plexiform layer (IPL) 30 days after transplantation. However, numerous ES cells growing in the recipient mouse retina showed a teratoma-like morphology and high proliferative potential after 30 days post-transplantation (Hara et al., 2004b).

Folate antagonist methotrexate (MTX) is used as a chemotherapeutic agent in inducing clinical remission of intraocular malignant lymphoma and other intraocular malignancies, even in the presence of an aggressively growing tumor (Velez et al., 2001). Even a single intravitreal injection of MTX can lead to a tumor control lasting for a longer period than that achieved by systemic administration of MTX (de Smet et al., 1999).

Neural stem cells commonly fail to integrate within the retina after injections into the vitreous chamber of healthy rodents, while neural stem cells transplanted in the same way into rodents with retinas lesioned mechanically and/or with inherited retinal degeneration exhibit retinal incorporation (Meyer et al., 2006; Nishida et al., 2000). Retinal ganglion cells are exquisitely sensitive to the effects of glutamate and its analog N-methyl-D-aspartate (NMDA), which produces a dose-dependent cell damage both in vivo and in vitro, and glutamate toxicity has been implicated in the pathophysiology of glaucoma (Hara et al., 2004a; Kumada et al., 2005). Thus, NMDA-treated mouse is a good model for cell-replacement therapy of retina.

In the present study, we apply a single intravitreal administration of MTX to control the neoplastic potentials of ES cells transplanted in the retinal ganglion-cell-damaged model of adult mouse, which is induced by intravitreal NMDA injection (Hara et al., 2004a; Kumada et al., 2005).

2. Results

2.1. *Incorporation of transplanted ES cells*

The incorporation of transplanted ES cells in MTX-treated and non-treated retinas at 4 weeks after transplantation was observed in 8/16 eyes (50%) and 8/16 eyes (50%), respectively. All the transplanted ES cells in both MTX-treated and non-treated retinas showed positive staining reactions revealed by immunohistochemical examination for GFP using an anti-GFP antibody (Figs. 1C and D). These ES cells on the serial histological sections also demonstrated green fluorescent signals by fluorescent microscopy (Figs. 1E and F).

2.2. *Morphology of transplanted ES cells*

By a conventional hematoxylin and eosin (HE) staining, the transplanted ES cells in MTX-treated retinas showed the tendency of differentiated morphology to the neuronal structures (Figs. 2A and B). These ES cells resembled a human benign brain tumor, gangliocytoma, which is recognized as a cluster of mature hamartomatous neuronal cells (Moreno et al., 2001). However, the transplanted ES cells in non-MTX-treated retinas exhibited larger part of the area with undifferentiated cell morphology than MTX-treated retinas. These undifferentiated cells often showed the primitive

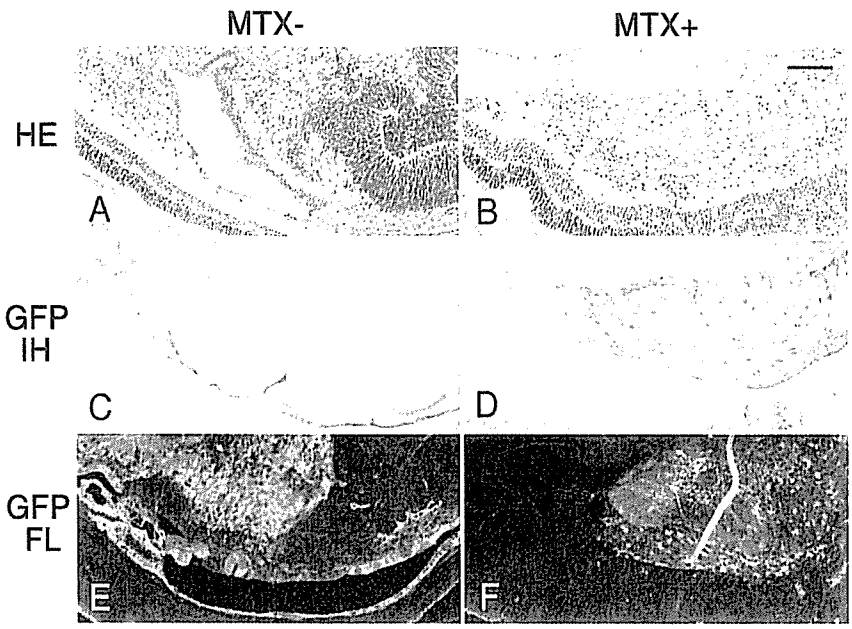

Fig. 1 – Representative microphotograph of transplanted ES cells in MTX-treated and non-treated retina. (A, B) Histological examination via hematoxylin and eosin staining. (A) Non-MTX-treated retina. Transplanted ES cells form primitive neuroepithelial structures associating mature gland tissues. (B) MTX-treated retina. Transplanted ES cells in MTX-treated retinas showed the differentiated morphology to the neuronal structures. (C, D) GFP immunohistochemistry of the transplanted tissues. Transplanted ES cells both in non-MTX-treated (C) and in MTX-treated retina (D) show brown-colored immunoreactivity for GFP. (E, F) Fluorescent signals for GFP. Green fluorescent signals produced by GFP in ES cells were detected both in non-MTX-treated (E) and in MTX-treated retina (F). Scale bar in panel B, 100 μm. (For interpretation of the references to colour in this figure legend, the reader is referred to the web version of this article.)

neuroepithelial structures (medulloepithelial rosettes) resembling neural tubes (Figs. 1A and 3A).

2.3. *Neuronal differentiation and teratogenic potential*

The results of the immunohistochemical examination for neuronal and teratogenic potential were summarized in Tables 1 and 2.

In this study, the neuronal differentiation was expressed by the neuronal index of each neuronal marker. The immunostaining intensity (ISI) of each neuronal marker expressed by ES cells was assessed semi-quantitatively by microscopic examination as follows: negative, 0; weakly positive, 1; positive, 2; and strongly positive, 3. Each neuronal index is defined as the product of ISI by the ratio of the area expressing each neuronal marker to all the area of transplanted ES cells. Student's *t* test was used to compare the difference between MTX-treated group and non-treated group. P value of less than 0.05 is considered statistically significant.

In the 6 neuronal markers such as protein kinase C (PKC), syntaxin, β-tubulin, vesicular glutamate transporter 1 (VGLUT1), neurofilament protein (NFP) and synaptophysin and a glial cell marker, glial fibrillary acidic protein (GFAP) (Figs. 2C to P), there was a significant difference in the index scores of PKC, syntaxin and NFP between MTX-treated and non-treated retina ($P < 0.05$). β-tubulin, VGLUT1 and synaptophysin also showed the tendency exhibiting high neuronal index in MTX-treated retina. Among these 7 markers, only GFAP was expressed evenly in MTX-treated and non-treated retina.

Teratogenic potential was evaluated as positive even if a small area of the transplanted ES cells was weakly positive for a teratogenic marker. Fisher's exact probability test was used for statistical analysis to compare frequencies. *P* value of less than 0.05 is considered statistically significant. In the 5 teratogenic markers for α-fetoprotein (AFP), vimentin, cytokeratin AE1/AE3 (CK), placental alkaline phosphatase (PLAP) and chorionic gonadotropin (Figs. 3B to F) showed significant difference in their expression between MTX-treated and non-treated retina. There was no AFP expression in ES cells of MTX-treated retina, whereas 5 out of 8 cases in non-treated retina expressed AFP ($P < 0.01$). There was only one case expressing vimentin in MTX-treated retina, whereas 5 out of 8 cases expressing vimentin in non-treated retina ($P < 0.05$).

The results of the immunohistochemical examination revealed that ES cells in MTX-treated retina, compared with non-MTX-treated retinas, showed increased neuronal differentiation in contrast to decreased expression of teratogenic markers. ES cells in non-MTX-treated retina showed decreased neuronal differentiation and increased expression of teratogenic marker.

2.4. *Proliferative activity of the transplanted ES cells*

Proliferative activity of the transplanted ES cells was evaluated by three independent methods, mitotic index by HE staining, PCNA index by immunohistochemistry and AgNOR count.

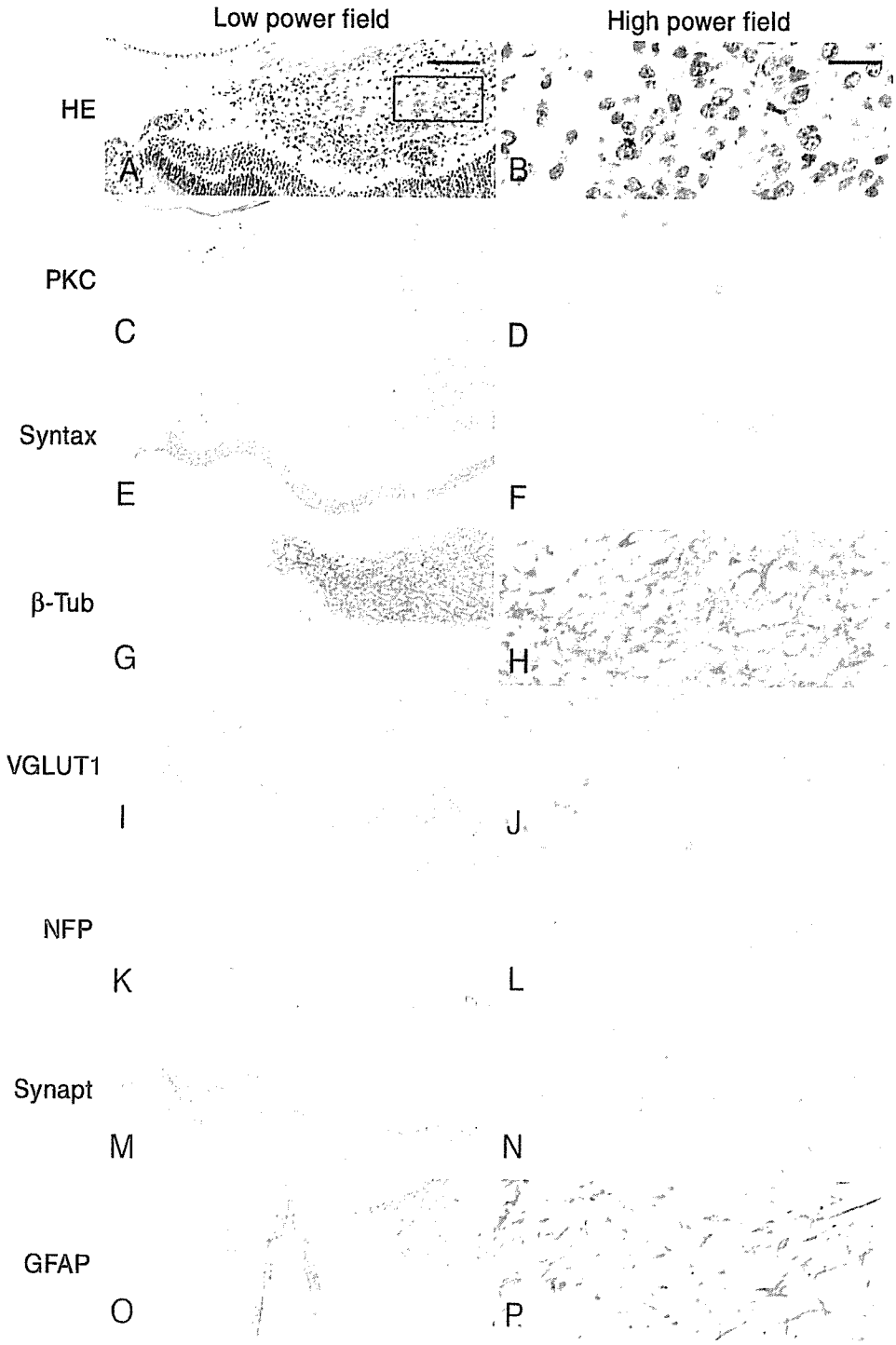

Fig. 2 – Conventional hematoxylin and eosin staining (A, B) and immunohistochemistry for protein kinase C (C, D), syntaxin (E, F), β-tubulin (G, H), VGLUT1 (I, J), neurofilament protein (K, L), synaptophysin (M, N) and glial fibrillary acidic protein (O, P) were analyzed to determine neuronal differentiation of the transplanted ES cells in an MTX-treated retina. Rectangle in panel A represents the area of high-power field in panel B. (A, C, E, G, I, K, M, O) Low-power field; (B, D, F, H, J, L, N, P) High-power field. HE, hematoxylin–eosin; PKC, protein kinase C; Syntax, syntaxin; β-Tub, β-tubulin; VGLUT1, vesicular glutamate transporter 1; NFP, neurofilament protein; Synapt, synaptophysin; GFAP, glial fibrillary acidic protein. Scale bar in panel A, 100 μm; scale bar in panel B, 30 μm.

Mitotic figures in sections stained with HE were counted through the microscope in 10 random high-power fields (×400). The PCNA index was defined as the percentage of PCNA positive cells in 1000 randomly selected ES cells under the same observation conditions. For judging positivity of immunostaining, only strong nuclear immunostaining was regarded as positive; weak nuclear staining was regarded as negative. The AgNORs were present as clearly visible black

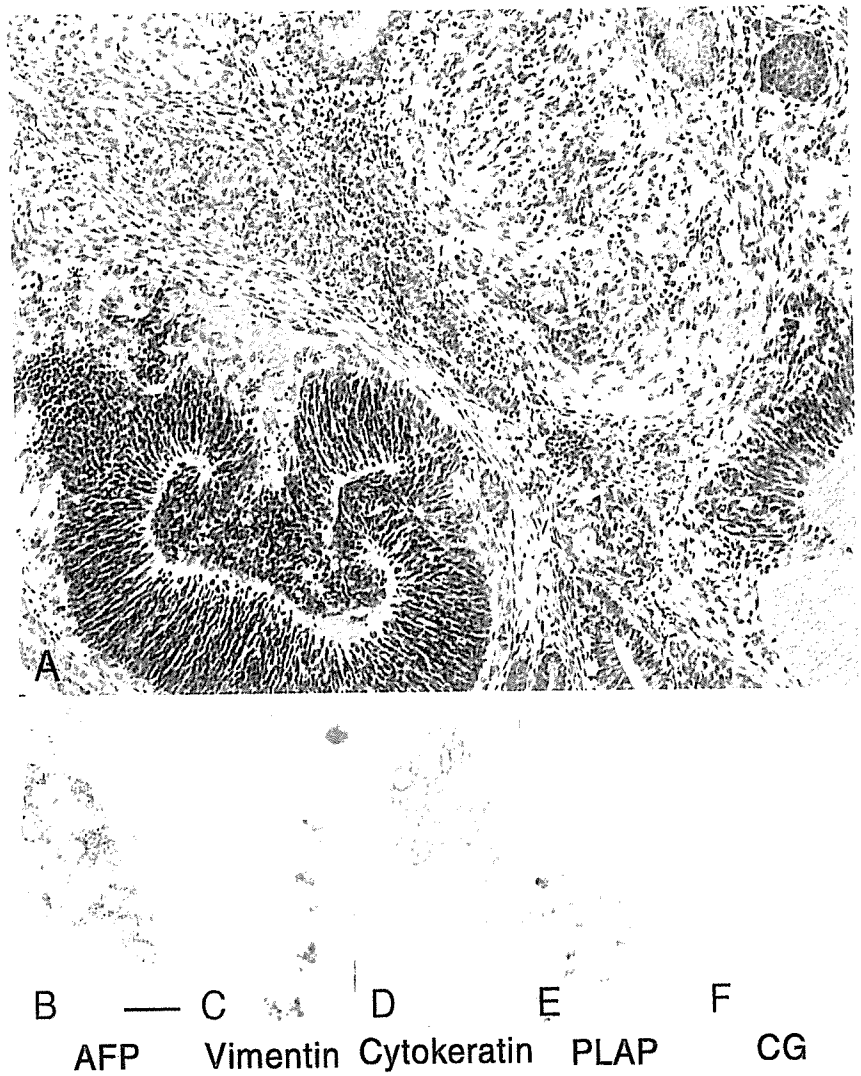

Fig. 3 – Representative microphotograph of immature teratoma arising from transplanted ES cells in non-MTX-treated retina. Conventional hematoxylin and eosin staining (A) and immunohistochemistry for α-fetoprotein (B), vimentin (C), cytokeratin AE1/AE3 (D), placental alkaline phosphatase (E) and chorionic gonadotropin (F) were analyzed to detect teratogenic potential of the immature teratoma. AFP, α-fetoprotein; PLAP, placental alkaline phosphatase; CG, chorionic gonadotropin. Scale bar in panel B, 30 μm.

dots in the cell nuclei. In oncology, a number of studies carried out in different tumor types demonstrated that malignant cells frequently present a greater amount AgNOR protein than corresponding non-malignant cells (Trere, 2000). The mean number of AgNORs in a total of 200 ES cells nuclei was calculated in each case. These methods, mitotic index, PCNA index and AgNOR count, were performed by a blinded trained histopathology technician.

Student's t test was used to compare the difference between MTX-treated group and non-MTX-treated group. P value of less than 0.05 is considered statistically significant.

The results of the proliferative activity of transplanted ES cells in MTX-treated and non-treated retina were summarized in Table 3. Mitotic index and AgNOR count demonstrated that proliferative activity of ES cells in MTX-treated retina is significantly lower than that in non-MTX-treated retina. Mitotic index in MTX-treated retina was 0.31 ± 0.44 and that in non-MTX-treated retina was 1.76 ± 1.39 ($P < 0.05$). AgNOR count in MTX-treated was 1.82 ± 0.53 and that in non-MTX-treated retina was 2.85 ± 0.69 ($P < 0.01$). PCNA index also showed the tendency of low cell proliferation in MTX-treated retina (9.99 ± 8.45) compared with non-MTX-treated retina (20.93 ± 18.49).

3. Discussion

In the present study, expression of PKC, syntaxin, β-tubulin, VGLUT1, NFP, synaptophysin and GFAP, which are all expressed as neuronal and glial cell markers in normal adult retina (Hara et al., 2004b; Marquardt et al., 2001; Sherry et al., 2003), was analyzed in transplanted ES cells in mouse retina. There was a significant difference in the expression of PKC, syntaxin and NFP between MTX-treated and non-treated retina. Furthermore, β-tubulin, VGLUT1 and synaptophysin also showed a tendency of neuronal

Table 1 – Neuronal differentiation indexes[a] of each neuronal marker in MTX-treated and non-treated ES cells transplanted in adult mouse retina

Retina ID	PKC	Syntax	β-Tub	VGLUT1	NFP	Synapt	GFAP
				MTX(+)			
1	1	0.3	0.4	0.2	1	0.3	0.2
2	2	0.9	0	0	0.8	0.8	0.8
3	2	2	3	1	2	3	0.3
4	0.1	0.1	0.3	0.9	0.8	0	0.2
5	1	0.8	1.2	0.5	0.8	0.8	0.3
6	2.7	1.6	1	1.8	1.8	0.3	0.3
7	2.7	1.5	1.5	1.8	2.4	1.6	2.4
8	1.8	1.8	0.4	0.5	0.8	0.5	0.5
Mean ± SD	1.66 ± 0.9	1.13 ± 0.7	0.98 ± 0.96	0.84 ± 0.68	1.30 ± 0.66	0.91 ± 0.97	0.63 ± 0.74
				MTX(−)			
9	0.9	0	0	0.1	0	0	0
10	0.3	0.1	0.3	0.2	0.2	0.1	0.3
11	0	0	0	0.2	0.2	0	0.3
12	0.8	0.4	0.9	0.5	0.3	0.3	0.6
13	1.4	0.6	0.9	0.5	0.3	0.6	0.3
14	0.7	0	0.1	1	0.5	0	0.5
15	1.6	1.6	2.1	0.7	1.4	0.7	2.1
16	0.6	0.4	0.6	0.9	1.8	0.4	0.9
Mean ± SD	0.79 ± 0.53	0.39 ± 0.54	0.61 ± 0.71	0.51 ± 0.34	0.59 ± 0.65	0.26 ± 0.28	0.63 ± 0.65
P value	0.034	0.033	0.4	0.24	0.048	0.09	1

P value of less than 0.05 is considered statistically significant.

PKC, protein kinase C; Syntax, syntaxin; β-Tub, β-tubulin; VGLUT1, vesicular glutamate transporter 1; NFP, neurofilament protein; Synapt, synaptophysin; GFAP, glial fibrillary acidic protein.

[a] The values of the neuronal differentiation indexes are described in Results.

differentiation in MTX-treated retina. In the teratogenic markers, AFP and vimentin showed significant differences in their immunostaining reactivities between MTX-treated and non-treated retina. These results show that intravitreal administration of MTX increases neuronal differentiation and decreases expression of teratogenic markers in transplanted ES cells. Furthermore, three independent methods, mitotic index by HE staining, PCNA index by immunohistochemistry and AgNOR count, demonstrated the decrease of proliferative activity of transplanted ES cells by the treatment with MTX. Thus, our results suggest that intravitreal MTX treatment can induce neuronal differentiation in the transplanted ES cells and reduce their proliferative activity.

Many studies have demonstrated that neural progenitor cells possess at least partial ability to regenerate and repair neuronal damage within the central nervous system (CNS). Since retina is an essential neural compartment, it can be used experimentally for understanding the regeneration of the CNS. The in vivo application of neural progenitor cells obtained from donor animals for cell-replacement therapy is limited because of a scarcity of suitable neural progenitor cell populations which can be transplanted into the retina (Pressmar et al., 2001; Warfvinge et al., 2001; Wojciechowski et al., 2002). Furthermore, when neural progenitor cells are transplanted into murine retinas, their differentiation into mature neurons is limited, and they fail to differentiate into retina-specific neuronal elements (Nishida et al., 2000; Takahashi et al., 1998). Thus, the use of neural progenitor cells obtained from donor animals is not a good solution for cell-replacement therapy models. These specific cell populations can be obtained in huge quantities by differentiating embryonic stem cells into the respective neural precursor cells. ES cells may provide a putative new source of differentiated cell types for cell-replacement therapy (Keller, 2005), however, even neural precursor cells derived from ES cells show the unlimited self-renewal and high differentiation potential into various cell types and have the risk of tumor induction after engraftment (Arnhold et al., 2004).

Essentially, in vivo application of undifferentiated ES cells into immune-deficient mice produces teratomas comprised of many cell types (Bieberich et al., 2004) and the integrated ES cells into retina also have a tumorigenic effect (Hara et al., 2004b). Thus, control of proliferative activity and maintenance of neuronal differentiation in the transplanted ES cells is considered very important since the transplanted ES cells may be a therapeutic option for patients with degenerative or injured disease in the future.

MTX is clinically used for its anti-inflammatory actions in the treatment of rheumatoid arthritis (van Ede et al., 1998). It is reported that the anti-inflammatory effects of MTX are mediated by adenosine production in inflammatory sites. Cronstein et al. (1993) demonstrated the anti-inflammatory effects of methotrexate result from its capacity to promote intracellular accumulation of 5-aminoimidazole-4-carboxamide ribonucleotide (AICAR) that, under conditions of cell injury, increases local adenosine release in the murine air pouch model. Pharmacologically relevant doses of methotrexate increased splenocyte AICAR

Table 2 – Teratogenic potential evaluated by each teratogenic marker in MTX-treated and non-treated ES cells transplanted in adult mouse retina

Retina ID	AFP	Vimentin	CK	PLAP	CG
			MTX(+)		
1	–	+	+	–	+
2	–	–	–	–	–
3	–	–	+	–	–
4	–	–	–	–	–
5	–	–	+	+	+
6	–	–	–	+	–
7	–	–	+	–	–
8	–	–	+	–	–
Case no. (%)	0 (0%)	1 (12.5%)	5 (62.5%)	2 (25%)	2 (25%)
			MTX(–)		
9	–	–	–	–	–
10	+	+	+	+	+
11	–	+	+	+	+
12	+	+	+	+	+
13	+	+	–	–	–
14	–	–	+	–	–
15	+	+	+	–	+
16	+	–	–	–	–
Case no. (%)	5 (62.5%)	5 (62.5%)	5 (62.5%)	3 (37.5%)	4 (50%)
P value	0.007	0.039	1.000	0.590	0.302

Teratogenic potential was evaluated as positive even if only a small area of the transplanted ES cells is weakly positive for a teratogenic marker. +, positive; –, negative. P value of less than 0.05 is considered statistically significant.
AFP, α-fetoprotein; CK, cytokeratin AE1/AE3; PLAP, placental alkaline phosphatase; CG, chorionic gonadotropin.

content, raised adenosine concentrations in exudates from carrageenan-inflamed air pouches and markedly inhibited leukocyte accumulation in inflamed air pouches (Cronstein et al., 1993). Their results indicate that MTX is a nonsteroidal anti-inflammatory agent that increases adenosine release at inflamed sites.

Interestingly, Bilodeau et al. (2005) reported recently that adenosine is a physiological signal in neuronal differentiation of the central-nervous-system-derived catecholaminergic cell line and suggest that adenosine signaling is involved in neural crest cell development and differentiation in vivo. Our results showed the induction of the neuronal differentiation and reduction of teratogenic and proliferative activity of the transplanted ES cells in mouse adult retinas with a single intravitreal administration of MTX. Thus, the findings of the present study suggest that adenosine plays some role in the induction of neuronal differentiation in MTX-treated ES cells in retina. On the other hand, MTX is reported to induce differentiation of human epidermal keratinocytes in vitro (Schwartz et al., 1992). MTX inhibits proliferation of keratinocytes and also induces several markers of differentiation. The effects of MTX seem to have low cytotoxicity since keratinocytes not only remain viable but also actively synthesize proteins (Schwartz et al., 1992). Furthermore, MTX modifies osteoblast-specific key genes on differentiating mouse ES cells into skeletal system (Pellizzer et al., 2004).

Intrathecal chemotherapy with MTX for medical treatment as an antineoplastic agent is safely utilized even in children with leukemia and lymphoma, and in some brain tumors, compared with other chemotherapeutic agents (Ruggiero et al., 2001). Intravitreal chemotherapy with MTX is also effective in inducing clinical remission of intraocular malignant lymphoma and other intraocular malignancies, even in the presence of an aggressively growing tumor (Velez et al., 2001). Even a single intravitreal injection of MTX can lead to a tumor control lasting for a longer period than that achieved by systemic administration of MTX (de Smet et al., 1999). In the present study, the proliferative activity of transplanted ES cells in MTX-treated retina is significantly lower than that in non-MTX-treated retina by mitotic index and AgNOR count. PCNA index also showed the tendency of low cell proliferation in MTX-treated retina compared with non-MTX-treated retina. Thus, in our method, a single intravitreal injection of MTX is safe and convenient to control the proliferative activity of ES cells transplanted in retina and may be applied for clinical use in the future.

In conclusion, MTX, which is clinically applicable to intraocular administration, seems to be a very useful agent for cell-replacement therapy using ES cells in retina because of its low toxicity to a nervous system, its suppressive action as an anti-neoplastic drug against aggressively growing cells and its inducing ability of neuronal differentiation. Further studies are needed about the functional activity in the transplanted ES cells treated with MTX because our results revealed only the neuronal differentiation without structural recovery of a neuronal network of the retina.

Table 3 – Proliferative activities evaluated by mitotic index, PCNA index and AgNOR count in MTX-treated and non-treated ES cells transplanted in adult mouse retina

Retina ID	Mitotic index	PCNA index	AgNOR count
		MTX(+)	
1	1.16	17.05	3.08
2	0	2.52	1.46
3	0	ND	1.92
4	0	25.3	1.64
5	0.78	7.67	1.48
6	0.36	5.1	1.59
7	0.2	10	1.72
8	0	2.3	1.68
Mean ± SD	0.31 ± 0.44	9.99 ± 8.45	1.82 ± 0.53
		MTX(–)	
9	1.15	9.05	2.15
10	2.16	32.61	2.86
11	0.23	6.95	2.47
12	4.37	61.62	3.44
13	2.2	19.48	3.71
14	0.92	12.2	2.6
15	2.7	17.95	3.68
16	0.34	7.58	1.91
Mean ± SD	1.76 ± 1.39	20.93 ± 18.49	2.85 ± 0.69
P value	0.0227	0.159	0.0052

P value of less than 0.05 is considered statistically significant.

4. Experimental procedures

4.1. *Preparation and maintenance of GFP expressing ES cell line*

D3 ES cell or its derivative stably expressing enhanced green fluorescent protein (EGFP) was prepared as described previously (Hara et al., 2004b; Yamane et al., 1997). cDNA encoding enhanced green fluorescent protein (EGFP) was placed under the CAG promoter of the pCXN2 vector, in which the neo^r sequence was inserted into the pCAGGS expression vector. The D3 ES cells were transfected with the DNA by electroporation. Briefly, Dulbecco's modified essential medium (DMEM; GIBCO-BRL, Grand Island, NY) was supplemented with 15% fetal calf serum (FCS; Whittaker, MD), 1× nonessential amino acids (GIBCO-BRL), 0.1 mM 2-mercaptoethanol (Wako Pure Chemical Industries, Ltd, Osaka Japan) and a culture supernatant from CHO cells producing leukemia inhibitory factor (LIF; a gift from Genetics Institute inc., Cambridge, MA).

4.2. *Animals and experimental procedures*

Male ddY mice weighing 25–30 g were purchased from a local supplier (Chubukagakusizai, Co., Japan) and used in this study. All experimental manipulations were carried out under anesthesia induced by intraperitoneal injections of 50 mg/kg pentobarbital sodium (Nembutal, Dainippon Pharmaceuticals Co. Ltd., Japan). Animals were placed in the pronate position. Pupils were then dilated with one drop of 0.5% phenylephrine hydrochloride–0.5% tropicamide solution (Mydrin P, Santen Pharmaceutical, Japan). Using a 30-gauge needle, 2 μl of 10 mM NMDA (30 nmol) was intravitreally injected through the conjunctiva and sclera under erbinocular microscopy. Then, 2 μl of ES cell suspension (10^5 ES cells) in physiological saline was intravitreally injected 20 h after NMDA injection. After these treatments, one drop of ofloxacin ophthalmic solution (Tarivid topical solution, Santen Pharmaceutical, Japan) was applied to the eyes. One week after the ES cell injection, 2 μl of 5 mg/ml folate antagonist MTX in physiological saline was intravitreally injected in the same manner. The dose of MTX was based on published literature (de Smet et al., 1999; Ruggiero et al., 2001; Velez et al., 2001) and defined following a preliminary study. The vehicle was intravitreally injected as control in non-MTX-treated mice. Eyes were harvested 4 weeks after ES cell transplantation for histologic analysis.

4.3. *Histological examination*

Under deep anesthesia with sodium pentobarbital, animals were sacrificed by decapitation at 4 weeks after the ES cell transplantation. The eyes were enucleated and fixed in 10% formalin in phosphate-buffered saline overnight. Specimens were then embedded in paraffin. Horizontal sections were obtained through the optic nerve at 3 μm thick. Sections were stained with HE and underwent immunohistochemical analysis and green fluorescent signal detection.

4.4. *Confirmation of GFP of ES cell in the retina*

For the immunohistochemical confirmation of green fluorescent protein of ES cell in the retina, the deparaffinized sections were heated and boiled for 5 min by microwaving in 10 mM citrate buffer, pH 6.0. Expression of green fluorescent protein (GFP) in the transplanted ES cells was evaluated by treating samples with a rabbit polyclonal anti-GFP antibody (MBL Co. Ltd., Nagoya, Japan). The antibody at a dilution of 1:2000 in 0.05 M Tris-buffered solution, pH 7.6 (TBS), were added to the slides and incubated overnight at 4 °C. Expression of GFP was shown by the DAKO EnVision+ System, Peroxidase kit (K4003, DAKO, Carpinteria, USA). The peroxidase binding sites were detected by staining with 3,3′-diaminobenzidine. For the green fluorescent signal detection of the transplanted ES cells, the deparaffinized sections were immersed in phosphate buffer, and then green fluorescent signal was demonstrated by a fluorescent microscope using the excitation filter of 460–490 nm and barrier filter of 510 (Olympus Co. Ltd, Tokyo, Japan).

4.5. *Neuronal differentiation and teratogenic potential*

Expression of protein kinase C (PKC), syntaxin, β-tubulin, vesicular glutamate transporter 1 (VGLUT1), neurofilament protein (NFP), synaptophysin and glial fibrillary acidic protein (GFAP) were analyzed to determine neuronal and glial cell differentiation of the transplanted ES cells and incorporation into the retina. Anti-PKC (P5704, Sigma, St. Louis, USA), anti-syntaxin (S0664, Sigma), anti-β-tubulin (MMS-435P, Covance, Berkeley, USA), anti-VGLUT1 (135 002, Synaptic Systems, Goettingen, Germany), anti-NFP (NA 1297, Affiniti Research Products Ltd, Devon, UK), anti-synaptophysin (A0010, DAKO, Carpinteria, USA) and anti-GFAP (M0761, DAKO) antibodies used at a dilution of 1:500 (P5704), 1:1000 (S0664), 1:500 (MMS-435P), 1:2000 (135 002), 1:1000 (NA 1297), 1:200 (A0010) and 1:100 (M0761), respectively, in TBS were added to the slides and incubated overnight at 4°C. Teratogenic potential was also analyzed by immunohistochemistry for α-fetoprotein (AFP), vimentin, cytokeratin AE1/AE3 (CK), placental alkaline phosphatase (PLAP) and chorionic gonadotropin. Anti-AFP (A0008, DAKO), anti-vimentin (M0725, DAKO), anti-CK (M0630, DAKO), anti-PLAP (A268, DAKO) and anti-chorionic gonadotropin (A0231, DAKO) antibodies were also used at a dilution of 1:2000 (A0008), 1:200 (M0725), 1:100 (M0630), 1:500 (A268) and 1:2000 (A0231), respectively. Samples for PKC, syntaxin, synaptophysin, GFAP, vimentin and CK were heated and boiled for 5–10 min by microwaving in 10 mM citrate buffer, pH 6.0, before applying first antibodies. Expression of PKC, syntaxin, β-tubulin, GFAP, vimentin and CK was shown by the rabbit EnVision+ System, and that of VGLUT1, NFP, synaptophysin, AFP, PLAP, chorionic gonadotropin was done by Nichirei mouse-stain kit (Nichirei Co. Ltd, Tokyo, Japan).

4.6. *Analysis of the proliferative activity*

The proliferative activity of transplanted ES cells was detected by mitotic index by HE staining, proliferating cell nuclear antigen (PCNA) index by immunohistochemistry for PCNA

(DAKO M0879; used at a dilution of 1:400) and argyrophilic nucleolar organizer region (AgNOR) count. The AgNOR staining, described previously (Hara et al., 1991a, 1991b), is a useful and convenient tool for the evaluation of cellular proliferative activity. Briefly, deparaffinized sections were stained by a silver colloid technique for argyrophilic protein associated with nucleolar organizer regions. The silver colloid solution for AgNOR staining was prepared by dissolving gelatin in 1% aqueous formic acid at a concentration of 2%, and this solution was mixed, 1:2 by volume, with 50% aqueous silver nitrate (Hara et al., 1991b).

REFERENCES

Ahmad, I., Das, A.V., James, J., Bhattacharya, S., Zhao, X., 2004. Neural stem cells in the mammalian eye: types and regulation. Semin. Cell Dev. Biol. 15, 53–62.

Aoki, H., Hara, A., Nakagawa, S., Motohashi, T., Hirano, M., Takahashi, Y., Kunisada, T., 2006. Embryonic stem cells that differentiate into RPE cell precursors in vitro develop into RPE cell monolayers in vivo. Exp. Eye Res. 82, 265–274.

Arnhold, S., Klein, H., Semkova, I., Addicks, K., Schraermeyer, U., 2004. Neurally selected embryonic stem cells induce tumor formation after long-term survival following engraftment into the subretinal space. Invest. Ophthalmol. Visual Sci. 45, 4251–4255.

Bieberich, E., Silva, J., Wang, G., Krishnamurthy, K., Condie, B.G., 2004. Selective apoptosis of pluripotent mouse and human stem cells by novel ceramide analogues prevents teratoma formation and enriches for neural precursors in ES cell-derived neural transplants. J. Cell Biol. 167, 723–734.

Bilodeau, M.L., Ji, M., Paris, M., Andrisani, O.M., 2005. Adenosine signaling promotes neuronal, catecholaminergic differentiation of primary neural crest cells and CNS-derived CAD cells. Mol. Cell. Neurosci. 29, 394–404.

Cronstein, B.N., Naime, D., Ostad, E., 1993. The antiinflammatory mechanism of methotrexate. Increased adenosine release at inflamed sites diminishes leukocyte accumulation in an in vivo model of inflammation. J. Clin. Invest. 92, 2675–2682.

de Smet, M.D., Vancs, V.S., Kohler, D., Solomon, D., Chan, C.C., 1999. Intravitreal chemotherapy for the treatment of recurrent intraocular lymphoma. Br. J. Ophthalmol. 83, 448–451.

Doetschman, T.C., Eistetter, H., Katz, M., Schmidt, W., Kemler, R., 1985. The in vitro development of blastocyst-derived embryonic stem cell lines: formation of visceral yolk sac, blood islands and myocardium. J. Embryol. Exp. Morphol. 87, 27–45.

Fujikawa, T., Oh, S.H., Pi, L., Hatch, H.M., Shupe, T., Petersen, B.E., 2005. Teratoma formation leads to failure of treatment for type I diabetes using embryonic stem cell-derived insulin-producing cells. Am. J. Pathol. 166, 1781–1791.

Hara, A., Sakai, N., Yamada, H., Hirayama, H., Tanaka, T., Mori, H., 1991a. Nucleolar organizer regions in vascular and neoplastic cells of human gliomas. Neurosurgery 29, 211–215.

Hara, A., Sakai, N., Yamada, H., Yoshimi, N., Tanaka, T., Mori, H., 1991b. Rapid detection of proliferating potential in human brain tumors by nucleolar organizer region staining on squash preparations. J. Cancer Res. Clin. Oncol. 117, 510–514.

Hara, A., Niwa, M., Kumada, M., Kitaori, N., Yamamoto, T., Kozawa, O., Mori, H., 2004a. Fragmented DNA transport in dendrites of retinal neurons during apoptotic cell death. Brain Res. 1007, 183–187.

Hara, A., Niwa, M., Kunisada, T., Yoshimura, N., Katayama, M., Kozawa, O., Mori, H., 2004b. Embryonic stem cells are capable of generating a neuronal network in the adult mouse retina. Brain Res. 999, 216–221.

Haruta, M., Sasai, Y., Kawasaki, H., Amemiya, K., Ooto, S., Kitada, M., Suemori, H., Nakatsuji, N., Ide, C., Honda, Y., Takahashi, M., 2004. In vitro and in vivo characterization of pigment epithelial cells differentiated from primate embryonic stem cells. Invest. Ophthalmol. Visual Sci. 45, 1020–1025.

Keller, G., 2005. Embryonic stem cell differentiation: emergence of a new era in biology and medicine. Genes Dev. 19, 1129–1155.

Kumada, M., Niwa, M., Hara, A., Matsuno, H., Mori, H., Ueshima, S., Matsuo, O., Yamamoto, T., Kozawa, O., 2005. Tissue type plasminogen activator facilitates NMDA-receptor-mediated retinal apoptosis through an independent fibrinolytic cascade. Invest. Ophthalmol. Visual Sci. 46, 1504–1507.

Marquardt, T., Ashery-Padan, R., Andrejewski, N., Scardigli, R., Guillemot, F., Gruss, P., 2001. Pax6 is required for the multipotent state of retinal progenitor cells. Cell 105, 43–55.

Meyer, J.S., Katz, M.L., Maruniak, J.A., Kirk, M.D., 2004. Neural differentiation of mouse embryonic stem cells in vitro and after transplantation into eyes of mutant mice with rapid retinal degeneration. Brain Res. 1014, 131–144.

Meyer, J.S., Katz, M.L., Maruniak, J.A., Kirk, M.D., 2006. Embryonic stem cell-derived neural progenitors incorporate into degenerating retina and enhance survival of host photoreceptors. Stem Cells 24, 274–283.

Moreno, A., de Felipe, J., Garcia Sola, R., Navarro, A., Ramon y Cajal, S., 2001. Neuronal and mixed neuronal glial tumors associated to epilepsy. A heterogeneous and related group of tumours. Histol. Histopathol. 16, 613–622.

Nishida, A., Takahashi, M., Tanihara, H., Nakano, I., Takahashi, J.B., Mizoguchi, A., Ide, C., Honda, Y., 2000. Incorporation and differentiation of hippocampus-derived neural stem cells transplanted in injured adult rat retina. Invest. Ophthalmol. Visual Sci. 41, 4268–4274.

Okabe, S., Forsberg-Nilsson, K., Spiro, A.C., Segal, M., McKay, R.D., 1996. Development of neuronal precursor cells and functional postmitotic neurons from embryonic stem cells in vitro. Mech. Dev. 59, 89–102.

Pellizzer, C., Bello, E., Adler, S., Hartung, T., Bremer, S., 2004. Detection of tissue-specific effects by methotrexate on differentiating mouse embryonic stem cells. Birth Defects Res. B. Dev. Reprod. Toxicol. 71, 331–341.

Pressmar, S., Ader, M., Richard, G., Schachner, M., Bartsch, U., 2001. The fate of heterotopically grafted neural precursor cells in the normal and dystrophic adult mouse retina. Invest. Ophthalmol. Visual Sci. 42, 3311–3319.

Resnick, J.L., Bixler, L.S., Cheng, L., Donovan, P.J., 1992. Long-term proliferation of mouse primordial germ cells in culture. Nature 359, 550–551.

Ruggiero, A., Conter, V., Milani, M., Biagi, E., Lazzareschi, I., Sparano, P., Riccardi, R., 2001. Intrathecal chemotherapy with antineoplastic agents in children. Paediatr. Drugs 3, 237–246.

Schwartz, P.M., Barnett, S.K., Atillasoy, E.S., Milstone, L.M., 1992. Methotrexate induces differentiation of human keratinocytes. Proc. Natl. Acad. Sci. U. S. A. 89, 594–598.

Sherry, D.M., Wang, M.M., Bates, J., Frishman, L.J., 2003. Expression of vesicular glutamate transporter 1 in the mouse retina reveals temporal ordering in development of rod vs. cone and ON vs. OFF circuits. J. Comp. Neurol. 465, 480–498.

Soria, B., Skoudy, A., Martin, F., 2001. From stem cells to beta cells: new strategies in cell therapy of diabetes mellitus. Diabetologia 44, 407–415.

Takahashi, M., Palmer, T.D., Takahashi, J., Gage, F.H., 1998. Widespread integration and survival of adult-derived neural progenitor cells in the developing optic retina. Mol. Cell. Neurosci. 12, 340–348.

Takahashi, K., Mitsui, K., Yamanaka, S., 2003. Role of ERas in promoting tumour-like properties in mouse embryonic stem cells. Nature 423, 541–545.

Thomson, J.A., Itskovitz-Eldor, J., Shapiro, S.S., Waknitz, M.A., Swiergiel, J.J., Marshall, V.S., Jones, J.M., 1998. Embryonic stem cell lines derived from human blastocysts. Science 282, 1145–1147.

Trere, D., 2000. AgNOR staining and quantification. Micron 31, 127–131.

van Ede, A.E., Laan, R.F., Blom, H.J., De Abreu, R.A., van de Putte, L.B., 1998. Methotrexate in rheumatoid arthritis: an update with focus on mechanisms involved in toxicity. Semin. Arthritis Rheum. 27, 277–292.

Velez, G., Yuan, P., Sung, C., Tansey, G., Reed, G.F., Chan, C. C., Nussenblatt, R.B., Robinson, M.R., 2001. Pharmacokinetics and toxicity of intravitreal chemotherapy for primary intraocular lymphoma. Arch. Ophthalmol. 119, 1518–1524.

Warfvinge, K., Kamme, C., Englund, U., Wictorin, K., 2001. Retinal integration of grafts of brain-derived precursor cell lines implanted subretinally into adult, normal rats. Exp. Neurol. 169, 1–12.

Wojciechowski, A.B., Englund, U., Lundberg, C., Wictorin, K., Warfvinge, K., 2002. Subretinal transplantation of brain-derived precursor cells to young RCS rats promotes photoreceptor cell survival. Exp. Eye Res. 75, 23–37.

Yamane, T., Kunisada, T., Yamazaki, H., Era, T., Nakano, T., Hayashi, S.I., 1997. Development of osteoclasts from embryonic stem cells through a pathway that is c-fms but not c-kit dependent. Blood 90, 3516–3523.

Current Eye Research, 31:273–283, 2006

ISSN: 0271-3683 print / 1460-2202 online
DOI: 10.1080/02713680500536647

Taylor & Francis
Taylor & Francis Group

A New Calcium Channel Antagonist, Lomerizine, Alleviates Secondary Retinal Ganglion Cell Death After Optic Nerve Injury in the Rat

Md. Zahidul Karim,
Akira Sawada,
Hideaki Kawakami,
and Tetsuya Yamamoto
Department of Ophthalmology, Gifu University Graduate School of Medicine, Gifu, Japan

Takazumi Taniguchi
Glaucoma Group, Research and Development Center, Santen Pharmaceutical Co., Ltd., Nara, Japan

ABSTRACT *Purpose*: We investigated whether lomerizine, a new diphenylmethylpiperazine calcium channel blocker, exerted a neuroprotective effect on axonal or retinal damage induced by optic nerve injury in the rat. *Methods*: A partial crush lesion was inflicted unilaterally on the optic nerve, 2 mm behind the globe, in adult Wistar albino rats. Animals were treated with the vehicle, 10 or 30 mg/kg lomerizine. Each solution was given orally twice daily for 4 weeks. One week before euthanization, Fluoro-Gold (FG) was injected into both superior colliculi to retrogradely label surviving retinal ganglion cells (RGCs). Approximately 1 month after the optic nerve injury, the retinal damage was assessed morphologically, and the optic nerve axons surrounding the initial lesion were examined histologically. *Results*: The mean RGC density in the control group decreased to 65.9 ± 1.32% of the contralateral eye, whereas the systemic application of 10 or 30 mg/kg of lomerizine significantly enhanced the RGC survival to 88.1 ± 0.38% and 89.8 ± 0.28%, respectively. Histological examination of damaged axons revealed no significant enhancement of the density or total number of axons of the retinal ganglion cells in the lomerizine-treated group. The crush force we employed caused no significant morphological differences in the retinal layers between the sham-operated animals and the animals from the experimental groups. *Conclusions*: Our findings suggest that lomerizine alleviates secondary degeneration of RGCs induced by an optic nerve crush injury in the rat, presumably by improving the impaired axoplasmic flow.

KEYWORDS calcium channel blocker; lomerizine; neuroprotection; optic nerve injury; retinal ganglion cell

Received 19 February 2005
Accepted 15 December 2005

Correspondence: Dr. Md. Zahidul Karim, Ph.D., Department of Ophthalmology, Gifu University Graduate School of Medicine, 1-1 Yanagido, Gifu-city 501-1194, Japan. E-mail: karim-gif@umin.ac.jp

INTRODUCTION

Glaucoma is a common cause of visual impairment worldwide and may result in severe visual field loss. It is clinically characterized by retinal ganglion cell (RGC) death and unique patterns of visual field defects corresponding to optic

nerve head excavation. The progression of glaucoma can be slowed by reducingintraocular pressure (IOP) via medical or surgical intervention. However, in some cases the patient's condition deteriorates despite the clinician's therapeutic efforts.

The irreversible nature of RGC death is a consequence of axonal injury. Although the precise pathway by which glaucoma induces axonal injury is still controversial, much evidence has been accumulating that the neuroretinal damage occurs as a result of the toxic effects of free radicals, lipid peroxidation, and secretion of excitotoxic cellular mediators, most notably glutamate, after ischemic injury.[1–3] Glutamate is the principal excitatory neurotransmitter in the vertebrate retina used by photoreceptors, bipolar cells, and ganglion cells,[4] and it is intrinsically abundant in neurons. Glutamate is well-known to have a dual role: as an excitatory neurotransmitter under normal conditions[5,6] and as a toxin to neuronal cells under pathological conditions such as hypoxia, ischemia, and elevated intraocular pressure.[7] Furthermore, high glutamate concentrations are known to activate several types of cell surface receptors, including *N*-methyl-D-aspartate (NMDA) receptors, which interact at the neuronal membranes and activate Ca^{2+} channels.[8] In turn, they trigger the activation of a cascade starting with the intracellular migration of Ca^{2+} and leading to cellular apoptosis and necrosis in neural tissue.[1,8] From the view of the glutamate-Ca^{2+} overload neurotoxicity hypothesis, the inhibition of an influx of excess Ca^{2+} into neurons is a potential therapeutic opportunity for neuroprotection.

The Ca^{2+} antagonists are a group of drugs that were initially developed for use in the management of angina pectoris. Since their introduction, they have had a major impact in the therapy of patients with cardiac and vascular diseases. Calcium channel blockers reduce vascular tone by inhibiting the entry of calcium ions intracellularly, thus causing relaxation of the vascular smooth muscle cells. The vasodilatation has been shown to increase regional blood flow in several organs.[9,10] During the past three decades, calcium antagonists have been studied for their efficacy in the management of normal-tension glaucoma (NTG), which is a disease entity characterized by progressive optic nerve damage and visual field deficit, even in the absence of elevated intraocular pressure. Several investigators have reported favorable effects of Ca^{2+} channel blockers on the visual field deterioration in eyes with NTG, although others remain skeptical.[11] Although one of the major positive mechanisms of Ca^{2+} channel blockers in glaucoma is a putative improvement in blood supply around the optic nerve head,[11] the exact mechanism of this effect is still unknown.

1-[bis(4-Fluorophenyl)methyl] -4-(2,3,4-trimethoxybenzyl)-piperazine dihydrochloride (lomerizine) is a newly synthesized Ca^{2+} antagonist that was developed as a potential agent to improve the ocular or cerebrovascular circulation with minimum adverse cardiovascular effects.[12] Lomerizine specifically inhibits [^{3}H]nitrendipine binding to cerebral cortex membranes in the guinea-pig,[13] selectively inhibits the constriction of cerebral arteries induced by various stimulants *in vitro*,[14] and increases cerebral blood flow in cats.[15] Its effect on systemic blood pressure and heart rate is weaker than on the central nervous system (CNS) and cerebral arteries, suggesting that lomerizine might be more selective for the CNS and cerebral arteries than other known Ca^{2+} antagonists.[16] Furthermore, it has been reported that lomerizine inhibits both T- and L-type Ca^{2+} currents in single CA1 pyramidal cells of the rat hippocampus,[17] is effective at preventing glutamate-induced neurotoxicity in rat hippocampal cells in primary culture,[18] and exerts protective effects in animal models of ischemia and hypoxia.[19]

However, no data are available regarding the effect of lomerizine on secondary degeneration. Therefore, the current study investigated whether lomerizine has a neuroprotective effect in RGC degeneration induced by partial optic nerve injury in the rat.

MATERIALS AND METHODS

Animals

Male albino Wistar rats weighting between 240 and 310 g were used. All procedures were approved and monitored by the Animal Care Committee of the Gifu University Graduate School of Medicine, Japan, and were performed according to the procedures outlined in the ARVO statement for the Use of Animals in Ophthalmic and Vision Research. The rats were fed *ad libitum* and maintained in a temperature-controlled room on a 12-hr light/dark cycle (light period from 6 a.m. to 6 p.m.). All the procedures were conducted under general anesthesia using a mixture of ketamine hydrochloride (Fort Dodge Laboratories, Inc., Fort Dodge, LA, USA) and xylazine (Bitter, Columbus, OH, USA) injected intramuscularly.

Drug

Lomerizine hydrochloride was supplied by Nippon Organon (Osaka, Japan). The rats were randomly assigned to one of three groups and administered the vehicle, 10 or 30 mg/kg lomerizine. Lomerizine was dissolved in distilled water just prior to use and administered orally twice daily via a syringe in a concentration of 2 mg/ml (10 mg/kg) and 6 mg/ml (30 mg/kg) until euthanization. The vehicle-treated control rats were given an equal volume of distilled water in the same manner.

Optic Nerve Crush

With the aid of a binocular operating microscope, the conjunctiva of the right eye was incised laterally to the cornea, the retractor bulbi muscle was separated, and the optic nerve exposed by blunt dissection. The meninges were pierced and bluntly dissected with forceps. A cross-action calibrated forceps, size 60 gram (AM-1, experimental disposable clip, M·T Giken Co., Ltd, Tokyo, Japan), was placed approximately 2 mm posterior to the globe, and the optic nerve was partially crushed for 10 s. For the sham operation on the left eye, the same procedure was followed except that the optic nerve injury was not made. The retinal vasculature was checked using a direct ophthalmoscope immediately after the manipulations, and those animals with interrupted blood supply were excluded. The eyes were dressed with an 0.3% ofloxacin ophthalmic ointment (Tarivid; Santen, Osaka, Japan) until recovery.

Labeling of Retinal Ganglion Cells

Seven days before sacrifice, each rat was anesthetized and placed in a stereotactic apparatus. The skull was exposed and kept dry and clean. The bregma was identified and marked. A small window was drilled in the scalp at the following designated coordinates in the right and left hemispheres: at a depth of 4.5 mm from the surface of the skull, 6 mm behind the bregma on the anteroposterior axis, and 1.2 mm lateral to the midline. Using a Hamilton syringe, 1.5 μl of 2% Fluoro-Gold (FG: Fluorochrome Inc., Englewood, CO, USA) was slowly injected into the bilateral superior colliculi. The skin over the wound was then sutured, and antibiotic ointment was applied.

Assessment of RGC Survival

One week after the Fluoro-Gold injection, each rat was deeply anesthetized, and the eye was rapidly enucleated and fixed in 4% paraformaldehyde for 1 hr. The eye was bisected at the equator, the lens was removed, and the posterior segment was post-fixed for another 30 min. To prepare the flatmounts, the retina was dissociated from the underlying structures (sclera/choroid), flattened by six radial cuts, and then spread on a gelatin-coated glass slide. FG-labeled RGCs were visualized under a fluorescence microscope (Axioskop H, Carl Zeiss, Jenaer Germany) with a UV filter (blue-violet: 395–440 nm). Labeled RGCs were counted in 12 microscopic fields of the retinal tissue at 100× magnification obtained from three regions in each quadrant at two different eccentricities 1 mm (one field) and 4 mm (two fields) away from the optic disk. It has been reported that a retrogradely applied tracer would label not only RGCs but also microglia or macrophages that eventually phagocytosed degenerated or dead RGCs.[20] Therefore, we distinguished these cells morphologically and excluded them from further analysis. After preparing whole-mounts of retinae, FG-labeled RGCs were counted separately in each quadrant or eccentricity, and then the numbers were averaged. The survival rate of the RGCs was calculated as the percentage of the labeled RGCs in the crushed eye as compared with the uncrushed contralateral eye.

Histological Assessment of the Retina

Twenty-eight days after the optic nerve injury, the eye was enucleated under deep anesthesia. The globe was kept immersed for at least 24 hr at 4°C in a fixative solution containing 2.5% glutaraldehyde and 2% paraformaldehyde. Eight paraffin-embedded sections (thickness: 3 μm) cut through the optic disk of each eye were prepared in a standard manner and stained with hematoxylin and eosin. Histological changes in the retina were evaluated fundamentally as described by Honjo and associates,[21] three sections from each eye being used for the morphometric analysis. After light-microscopic images were taken, the number of cells, except displaced amacrine cells,[22] were counted in the ganglion cell layer (GCL), and the thickness of various retinal layers such as the inner plexiform layer (IPL), the inner nuclear layer (INL), and the outer nuclear

layer (ONL) were measured at a distance between 1 and 1.5 mm from the optic disk in a masked fashion. Data from three sections (selected randomly from the eight sections) were averaged for each eye and used to evaluate the cell count in the GCL and the thickness of each retinal layer. The data of the crushed eyes were expressed relative to the uncrushed contralateral eye.

Histological Examination of the Rat Optic Nerve

Both eyes in the vehicle-treated and 30 mg/kg lomerizine-treated groups were employed for the following histological examination of RGC axons. After the eyeball and optic nerve had been enucleated, a segment of the optic nerve from approximately 2 mm behind the globe was post-fixed by immersion in 2.5% glutaraldehyde and 2% paraformaldehyde in 10 mM PBS for at least 1 week at 4°C. After three washes with PBS, the nerve segment was immersed in 2% osmium tetroxide in saline for 2 hr and then washed again with PBS at room temperature. Subsequently, the segment was dehydrated in alcohol and embedded as a cross section in epoxy resin for sectioning. Cross sections (1 μm thick) were cut on an ultra-microtome, mounted on glass slides, and stained for myelin with 1% toluidine blue. For the measurement of the axon numbers, four central and four peripheral areas were randomly selected and photographed in each cross section of the optic nerve. In each area (3883.9 μm^2), every myelinated axon was counted, and the data from eight areas were averaged as the mean axon density. The area of the optic nerve cross-section was measured by outlining its border. The total number of axons was estimated from the mean axon density and the total optic nerve cross-sectional area. Photographs were obtained and axon numbers were counted in a masked fashion by a single observer.

Statistical Analysis

An analysis of variance (ANOVA) was used to determine the statistical significance of body weight. Additionally, a one-way ANOVA and post hoc comparisons based on Fisher's protected least significance difference were used to determine the statistical significance in RGC density and histological retinal thickness. A Mann-Whitney U test was employed for analysis of the density or number of RGC axons. A difference of $p < 0.05$ was considered significant.

RESULTS

Weight

Body weight increased gradually with time without regard to lomerizine administration, and at no point during follow-up was there a significant difference in weight among the control and lomerizine-treated groups (Kruskal-Wallis test; 28 days, $p = 0.7403$). Additionally, no side effect was observed in any animal throughout the follow-up period.

Effect of Lomerizine on RGC Survival

Figure 1 shows representative photographs from the three groups. In the crushed eye groups treated with 10 or 30 mg/kg lomerizine, substantially more RGCs were observed compared with the vehicle-treated crushed eye group. This finding was prominent especially in the peripheral retinal area. Table 1 and Figure 2 demonstrate the FG-labeled RGC density in the crushed and uncrushed eye groups and the survival rate 28 days after the optic nerve injury. The survival rate of RGCs in the control rats averaged 65.9 ± 1.32%. On the other hand, the mean survival rate in the 10 or 30 mg/kg lomerizine-treated groups was 88.1 ± 0.38% and 89.8 ± 0.28%, respectively ($p < 0.001$, one-way ANOVA).

We also explored the local distribution of FG-labeled RGCs. In the control group, the optic nerve injury induced more RGC death in the peripheral area (59.3 ± 2.3% of the contralateral uncrushed eye) than in the central area (70.0 ± 4.4% of the contralateral sham-operated eye). Regardless of the eccentricity (central and peripheral) or quadrant (temporal, upper, nasal, and lower), a similar enhancement in RGC density was associated with the application of 10 or 30 mg/kg of lomerizine ($p < 0.001$, control groups versus 10 or 30 mg/kg lomerizine-treated groups, Fisher's PLSD).

Histological Examination of Each Retinal Layer

Photomicrographs of the retinas of the vehicle-treated and lomerizine-treated rats are shown in Figure 3. In general, histological examination showed no significant structural changes in any retinal layer in any group. The number of RGCs identified in the GCL per section was 86.2 ± 4.1% in the vehicle-treated rats (n = 6), 97.4 ± 6.7% in the rats treated with 10 mg/kg lomerizine (n = 6), and 97.6 ± 13.4% in the rats treated with 30 mg/kg lomerizine (n = 5). The RGC

FIGURE 1 Fluorescence micrographs from representative regions of the whole-mounted rat retina. Micrographs in the central and peripheral areas were taken approximately 1 mm and 5 mm from the optic nerve head, respectively. To identify the tracer-labeled RGCs, Fluoro-Gold (FG) was injected bilaterally into the superior colliculi 3 weeks after a partial optic nerve crush. Scale bars indicate 100μm.

TABLE 1 FG-Labeled RGC Density 4 Weeks After Optic Nerve Injury in the Crushed and Uncrushed Eye Groups

	Control (n = 7)	10 mg/kg lomerizine (n = 8)	30 mg/kg lomerizine (n = 6)	p value
Crushed eyes	948.9 ± 72.2 (600.5–1102.4)	1249.1 ± 32.6 (1114.7–1361.8)	1235.6 ± 27.7 (1145.9–1309.2)	0.0005
		*	*	
Uncrushed eyes	1429.1 ± 45.0 (1257.9–1549.0)	1417.8 ± 30.6 (1237.9–1505.1)	1375.8 ± 32.2 (1265.1–1467.1)	0.5940
Survival rate (%)	65.9 ± 1.32	88.1 ± 0.38	89.8 ± 0.28	0.0000

RGCs/mm^2; mean ± SEM (range).
*$p < 0.001$, Fisher's PLSD.

numbers in the vehicle-treated group were not statistically significantly lower than those in the lomerizine-treated groups ($p = 0.6497$, one-way ANOVA).

The IPL thickness in the vehicle-treated group (107.5 ± 7.0%) was not significantly less than that in the lomerizine-treated groups (104.8±9.3% in the 10 mg/kg group and 94.9 ± 7.9% in the 30 mg/kg group). The INL in the vehicle-treated group (109.4 ± 2.9%) was not significantly thinner than that in the lomerizine-treated groups (107.5 ± 4.8% in the 10 mg/kg group and 103.8 ± 1.3% in the 30 mg/kg group). The mean thickness of the ONL in lomerizine-treated groups was

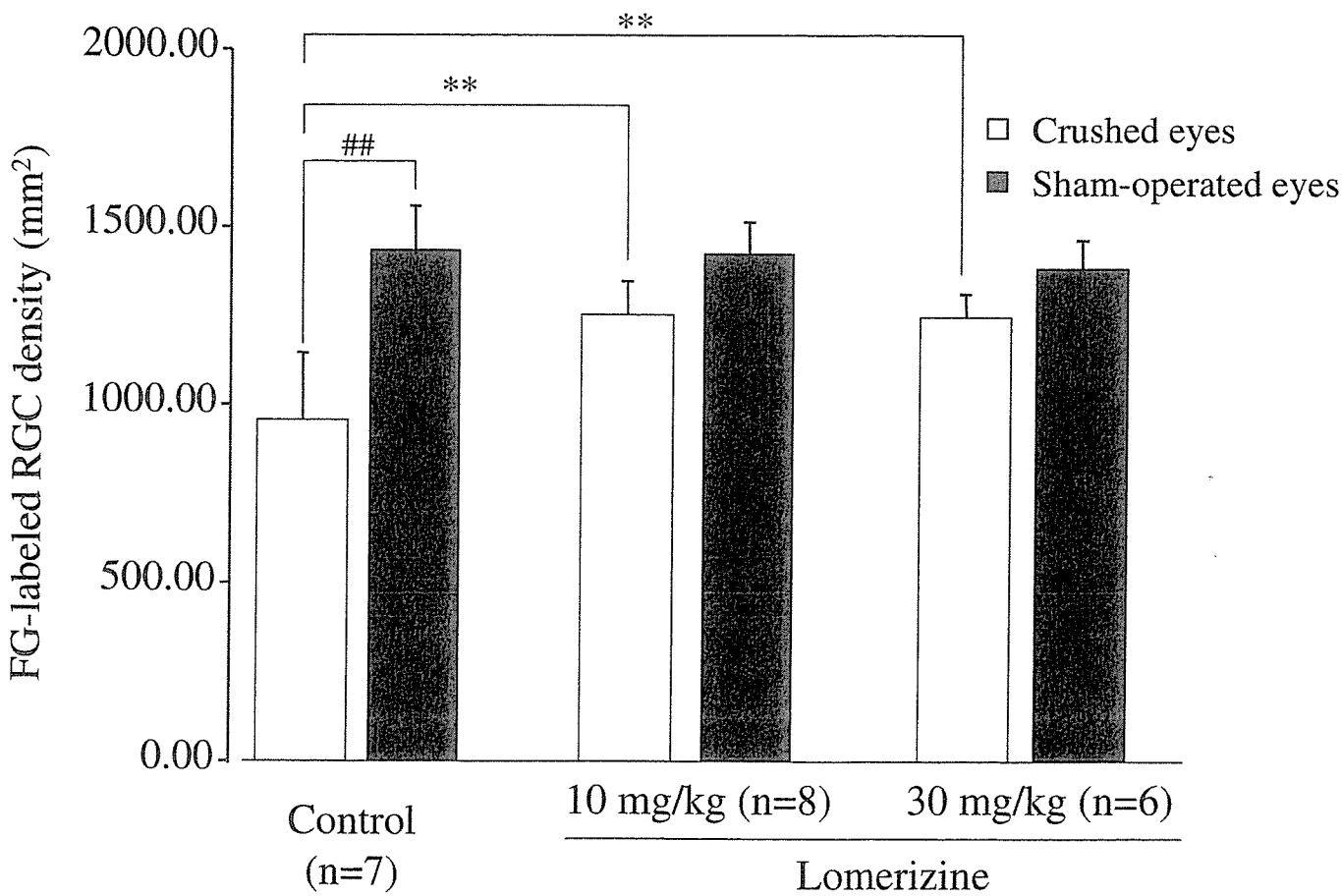

FIGURE 2 FG-labeled RGC density 4 weeks after optic nerve injury in the crushed and uncrushed eye groups. In the control group, there was a statistically significant difference in RGC density between the crushed and the contralateral uncrushed eye (##, $p = 0.0017$, Mann-Whitney *U* test). In the crushed eyes, there was a significant difference in RGC density among the control and 10 or 30 mg/kg lomerizine-treated groups ($p = 0.0005$, one-way ANOVA). Furthermore, the difference between the control group and the 10 or 30 mg/kg lomerizine-treated groups was significant (**, $p = 0.0003$, 0009, respectively, Fisher's PLSD). Error bars indicate SEM.

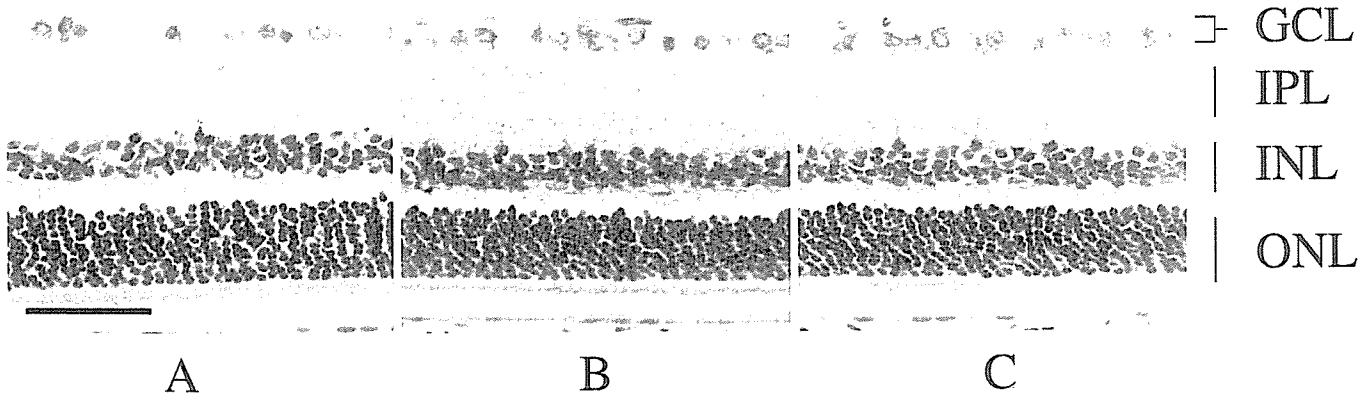

FIGURE 3 Light microscopic photographs of representative retinal cross-sections after optic nerve injury in the control and lomerizine-treated groups. (A) Crushed, with vehicle; (B) crushed, with 10 mg/kg lomerizine; (C) crushed, with 30 mg/kg lomerizine. GCL, ganglion cell layer; IPL, inner plexiform layer; INL, inner nuclear layer; ONL, outer nuclear layer.

107.5 ± 3.0% in the 10 mg/kg group and 96.2 ± 2.3% in the 30 mg/kg group. The ONL in the vehicle-treated group (99.2 ± 4.0%) was not significantly thinner than that in the lomerizine-treated groups.

Histological Changes in Axons of RGCs

In the cross section of the optic nerve, light microscopic examination revealed intact myelinated axons that had a regular arrangement in the contralateral sham-operated optic nerve of each group. Neither pathological nor remarkable axonal changes could be detected in the sham-operated axons. On the other hand, optic nerve crushing induced a decrease in the number of myelinated axons and an increase in connective tissue (by comparison with the sham-operated optic nerves) in both groups. Furthermore, the diameter of some axons was decreased in the crushed eye of both groups. Although the crushed axons in the 30 mg/kg lomerizine group preserved a relatively regular fiber arrangement, no fine arrangement was observed in the optic nerve (Fig. 4). In the optic nerve cross-sectional area, there were no significant differences in total axon numbers and axon density between the vehicle-treated and 30 mg/kg lomerizine-treated group.

DISCUSSION

In the current study, we demonstrated that long-term repeated administration of lomerizine exerted a neuroprotective effect against RGC degeneration after optic nerve crush injury in the rat. Moreover, this study found an increase in RGC body numbers without increases in the density or number of RGC axons, suggesting that this potential neuroprotective effect would be substantiated mainly by an improvement in retrograde axonal transport.

The actions of essential amino acids (EAAs), including glutamate-mediated neurotoxicity, are thought to be responsible for anoxic/ischemic, hypoglycemic, traumatic, and degenerative injuries to the central nervous system.[8] They may also play a pivotal role in the pathogenesis of glaucoma. In fact, glutamate has been identified as a major mediator of neuronal degeneration in the injured CNS, and elevated concentrations have been observed in glaucomatous human and monkey eyes.[23] Several Ca^{2+} antagonists have been reported to attenuate glutamate-mediated neurotoxicity in RGCs[24] and cortical cell cultures,[25] which strongly implicates the Ca^{2+} channels in glutamate-induced neurotoxicity. Lomerizine directly prevents glutamate-induced neurotoxicity in rat hippocampal primary cells.[18] Lomerizine also protects neuronal cells against retinal neurotoxicity both *in vivo* and *in vitro* by inhibiting the Ca^{2+} influx triggered by the activation of NMDA and non-NMDA receptors.[26]

Optic nerve crushing produces a graded, reproducible axonal injury that can be widely employed to explore alterations in RGCs.[27] This optic nerve injury is followed by chronic propagation of the damage; therefore, this model mimics the spreading of neurodegenerative diseases.[27] Actually, an Israeli group provided data showing that a controlled crush of the optic nerve resulted in a linear increase in the death of RGCs, and when NMDA antagonists were injected at some time point after the crush, then the death rate of ganglion cells was no longer linear but flattened out.[28] In the current study, we failed to observe any significant structural